Researchers Journal of Science and Technology (REJOST)

https://rejost.com.ng

Integrated Reservoir Characterization and Bypassed Hydrocarbon Evaluation for Optimized Recovery in 'UDEN' Field, Niger Delta, Nigeria

Ekong, Samuel Udo[1], George, Nyakno Jimmy[2], Udoh, Abraham Christopher[1], Ekefre, Anyanime Edet[1].

Abstract

Reservoir characterization and volumetric evaluation are central to defining the hydrocarbon potential and recovery strategy of producing fields. Although many Niger Delta studies have applied seismic attributes and petrophysical evaluation independently, fewer works have integrated deterministic reservoir characterization with probabilistic volumetrics to assess bypassed hydrocarbons. This study applies an integrated workflow combining three-dimensional (3D) seismic analysis, well log evaluation, and Monte Carlo simulation of Stock Tank Oil Initially in Place (STOIIP) to characterize the reservoir system and quantify bypassed hydrocarbon volumes in the Uden Field, Niger Delta, Nigeria. Three wells (UDEN-1, UDEN-2, and UDEN-3) along with a post-stack 3D seismic dataset were analyzed using Petrel 2014, Interactive Petrophysics, and Python-based stochastic modeling tools. Reservoir correlation delineated two sandstone units within the Agbada Formation, with average porosity of 0.25 – 0.29, permeability of 0.8 – 1.2 Darcy, and water saturation of 0.12 – 0.36. Seismic attribute analysis using RMS amplitude, maximum amplitude, and variance effectively delineated structural discontinuities and potential hydrocarbon accumulations. Deterministic mid-case STOIIP values for SAM-1 and SAM-2 were ~142 MMbbl, while Monte Carlo probabilistic simulation yielded P10, P50, and P90 estimates of 112, 142, and 177 MMbbl, respectively. Recovery factor estimates of 27 – 30% indicate remaining bypassed oil potential of up to ~121 MMbbl, supporting further infill drilling and recompletion opportunities. This integrated approach strengthens reservoir understanding and supports optimized recovery strategies in structurally complex Niger Delta settings.

✉ samuel4ekong@gmail.com

[1] Department of Geology, Akwa Ibom State University, Mkpat Enin, Uyo, Nigeria

[2] Department of Physics (Geophysics Research Group), Akwa Ibom State University, Mkpat Enin, Uyo, Nigeria

Keywords: Reservoir characterization; Seismic attributes; Bypassed hydrocarbons; Probabilistic volumetrics; Petrophysical evaluation; Niger Delta.

Article history
Received: October 2, 2025
Received in revised form: November 30, 2025
Accepted for publication: December 4, 2025
Available online: December 7, 2025

1.0 Introduction

Accurate reservoir characterization has become central to modern subsurface evaluation, and advances in seismic attribute analysis now play a pivotal role in enhancing the interpretation of reservoir geometry and fluid distribution. Seismic attributes derived from amplitude, frequency, and phase provide additional information beyond conventional structural interpretation, enabling improved detection of subtle stratigraphic and structural features (Chopra & Marfurt, 2007; Taner et al., 1979). These advances have transformed seismic data from a purely structural imaging medium into an indispensable tool for reservoir evaluation, capable of supporting predictions of lithology, porosity, and fluid content (Chopra & Marfurt, 2007; Gao, 2013; Udo et al., 2020; Ebong et al., 2023).

The Niger Delta Basin, one of Africa's most prolific hydrocarbon provinces, presents a complex interplay of stacked reservoirs, shale barriers, and fault-controlled compartmentalization (Evamy et al., 1978; Doust & Omatsola, 1990). The complexity of these reservoir systems often challenges traditional interpretation techniques and may result in undetected or under-drained zones. Previous studies have largely focused either on structural mapping or on petrophysical evaluation in isolation (Akpan et al., 2021). However, fewer studies have combined seismic attribute interpretation with both deterministic volumetrics and probabilistic modeling to explicitly screen for bypassed hydrocarbons in producing fields (Siddiqui et al., 2007; Fahrezi et al., 2022; Akpan et al., 2023). This represents a critical knowledge gap, particularly in matured fields where recovery optimization depends on identifying undrained compartments and subtle stratigraphic traps.

In this study, an integrated approach is applied to the Uden Field, utilizing 3D seismic attributes, well log interpretation, and Monte Carlo STOIIP simulations to characterize the reservoir system and evaluate the bypassed hydrocarbon potential. The study delineates reservoir continuity using log and seismic correlation, extract fluid-sensitive seismic attributes to identify amplitude - supported prospectivity, compute deterministic and probabilistic volumetric estimates, and quantify and evaluate remaining bypassed hydrocarbon volumes to support optimized field development (Akpan et al., 2020; Fahrezi et al., 2022).

2.0 Location and Geology of the Study Area

The Uden Field is located in the shallow offshore portion of the Niger Delta Basin, southern Nigeria (Fig. 1) and Fig 2 shows the well positions in the field. The Niger Delta lies between latitudes 4°N and 6°N, and longitudes 3°E and 9°E. It is one of the world's most prolific hydrocarbon provinces and represents a classic example of a passive margin deltaic system (Evamy et al., 1978; Doust & Omatsola, 1990). The basin is bounded by the Dahomey Embayment to the west, the Calabar Flank and Cameroon Volcanic Line to the east, and the Atlantic Ocean to the south, extending into the Gulf of Guinea.

The Niger Delta evolved during the Late Cretaceous to Recent, accumulating a thick sedimentary sequence exceeding 12 km in some depocenters (Tuttle et al., 1999), following the rifting and eventual separation of the South Atlantic during the Late Jurassic–Early Cretaceous (Burke et al., 1971; Akpan et al., 2023). The stratigraphic succession comprises three dominant formations deposited in a regressive sequence with Akata Formation

being the oldest and characterized by undercompacted marine shales with minor sandy interbeds, representing the prodelta facies. This unit serves as the principal petroleum source rock. The Agbada Formation follows this sequence and consists of alternating sandstone–shale sequences deposited in paralic to delta-front environments. The sandstone units constitute the major reservoirs, while the interbedded shales act as seals (Short & Stauble, 1967; Doust & Omatsola, 1990). Benin Formation is the youngest lithostratigraphic unit in the Basin. It is composed primarily of continental sands and gravels representing fluvial to upper delta plain deposits (Obianwu et al., 2015). Although generally non-prospective for hydrocarbons, it forms the region's major aquifer system.

These units define a characteristic coarsening-upward succession and form the essential lithostratigraphic framework of the Niger Delta petroleum system (Reijers, 1996). Basin architecture is heavily influenced by synsedimentary extensional tectonics, driven by rapid sediment loading and mobilization of over-pressured Akata shales. This has produced complex structural styles including listric growth faults, rollover anticlines, collapsed-crests, and shale diapirism (Weber & Daukoru, 1975; Morgan, 2004). These structures act as both migration pathways and trapping mechanisms, directly influencing reservoir distribution and compartmentalization (Umoren & George, 2018; Horsfall et al., 2024) For the Uden Field specifically, structural features including fault-assisted closures, rollover limbs, and antithetic fault splays control hydrocarbon trapping and accumulation. Understanding these geological and structural controls provides critical context for seismic attribute interpretation and reservoir prediction.

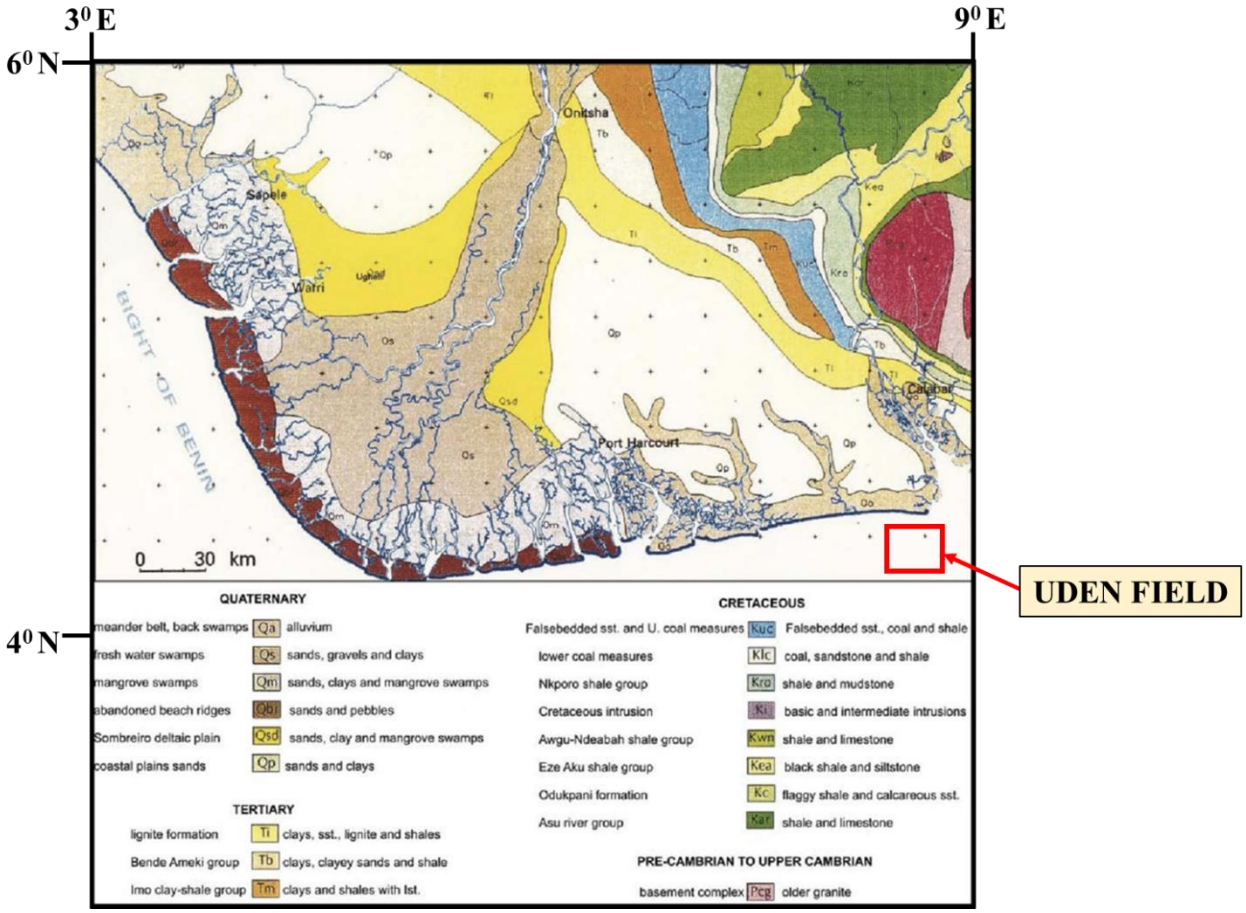

Fig 1: Geologic Map of Niger Delta showing field location (modified from Reijers (1996)

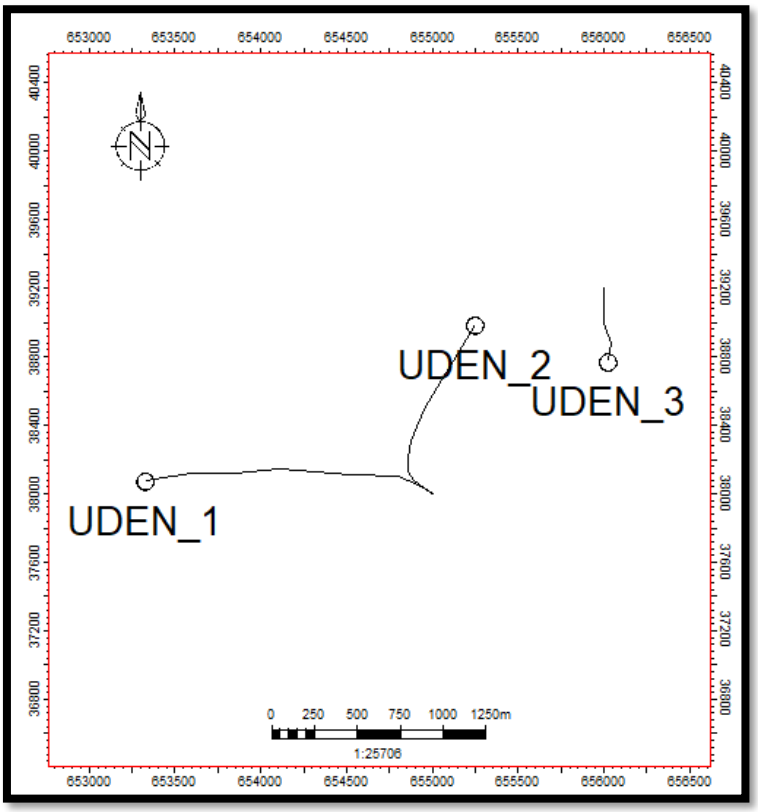

Fig 2: Base concession map of the field

3.0 Materials and Methods

This study integrates well logs and 3D seismic data to characterize the subsurface architecture, correlate reservoir intervals, and identify potential hydrocarbon-bearing zones within the Uden Field. Well heads, deviation surveys, check shots, and log suites (gamma ray, resistivity, neutron porosity, density, and sonic logs) were imported into Petrel 2014 to establish accurate spatial positioning and depth control. The logs were normalized using linear normalization to standard industry ranges (GR: 1 – 150 API; resistivity: 0.2 – 2000 Ωm; density: 1.65–2.65 g/cc; neutron porosity: 0–0.6 v/v; sonic: 40 – 140 µs/ft) to ensure uniform comparison and minimize tool-response bias.

Well correlation was performed along a strike section (M–M′) using gamma ray for lithological differentiation and resistivity for fluid characterization. Two reservoir tops and bases were correlated to define gross thickness, net-pay thickness, and lateral continuity.

Petrophysical analysis employed GR, resistivity, NPHI, and RHOB logs to compute key reservoir parameters. Porosity was determined from bulk density using Equation (1), shale volume from gamma ray index using Equation (2), and water saturation using Archie's relation in Equation (3). Hydrocarbon saturation (Sh = 1 − Sw) was derived using Equation (4), net-to-gross from Equation (5), while permeability was estimated using Timur's empirical equation in Equation (6).

$$\phi = \frac{\rho_{mat} - \rho_{bulk}}{\rho_{mat} - \rho_{fluid}} \quad (1)$$

where ρ_{mat} = Density of Rock Matrix, ρ_{bulk}= Bulk Density and ρ_{fluid}= Fluid Density

$$I_{GR} = \frac{GR_{Log} - GR_{min}}{GR_{max} - GR_{min}} \quad (2)$$

where I_{GR} = Gamma ray index, GR_{log} = Gamma ray reading of the Formation, GR_{min} = Minimum gamma ray (clean sand) and GR_{max} = Maximum gamma ray (shale).

$$S_W = \left(\frac{R_o}{R_t}\right)^{\frac{1}{n}} \quad (3)$$

where R_o= resistivity of rock filled with water, R_t= resistivity of suspected oil zone and n = saturation exponent (generally assumed to be 2)

$$S_h = 1 - S_w \quad (4)$$

where: Sh= hydrocarbon saturation and Sw = water saturation

$$NTG = \frac{Net\ Sand}{Gross\ sand} \quad (5)$$

$$k = 0.136 \times \emptyset^4 \times S_{wirr}^{-2} \quad (6)$$

where k represents an empirical constant dependent on lithology and irreducible water saturation, $\mathbf{S_{wirr}}$ is irreducible water saturation and $\emptyset$ is Porosity.

Seismic interpretation included synthetic seismogram generation and well-to-seismic calibration. Acoustic impedance was computed from calibrated sonic and density logs, reflection coefficients derived, and convolved with a statistical wavelet extracted from seismic traces around the wells. The well-seismic tie showed a correlation coefficient greater than 0.80, validating reflector alignment.

Faults were mapped on every inline and crossline, at 25 m line spacing, using reflection terminations, offsets, and amplitude discontinuities. Horizons were mapped at 5 ms sampling intervals, forming the basis for time-structure maps. Time maps were subsequently converted to depth using a velocity model calibrated with well check shot data.

Seismic attribute analysis employed variance, RMS amplitude, maximum amplitude, maximum magnitude, and average magnitude volumes to highlight structural discontinuities and amplitude anomalies (Ekanem et al., 2021; Akpan et al., 2025). RMS and maximum amplitude attributes were used to infer possible hydrocarbon-bearing zones, while variance aided in identifying sub-seismic scale faulting.

Volumetric analysis used both deterministic and probabilistic approaches. Deterministic STOIIP was estimated from reservoir properties using standard volumetric equations combining gross rock volume (GRV), net-to-gross (NTG), porosity (ϕ), water saturation (S_w), and formation volume factors. Probabilistic STOIIP estimation employed Monte Carlo simulations (10,000 iterations) in Python using NumPy, applying normally distributed parameters for porosity and water saturation (±10% standard deviation), and a triangular distribution for reservoir areal extent (P90–P50–P10 constraints derived from structural mapping). Resulting STOIIP probability distributions were analyzed using histogram and cumulative density functions to derive P10, P50, and P90 volume estimates.

Finally, bypassed hydrocarbon screening incorporated petrophysical cutoffs (porosity ≥ 0.20; Sw ≤ 0.35; NTG ≥ 0.60; net pay ≥ 20 ft) alongside production history to identify intervals likely to retain unrecovered hydrocarbons. Identified intervals were recommended for potential re-completion, infill drilling, or advanced reservoir monitoring.

4.0 Results and Discussion

Well correlation across UDEN-1, UDEN-2, and UDEN-3 demonstrates strong lateral continuity of both SAM-1 and SAM-2 reservoirs in the Agbada Formation (Fig. 3), indicating regionally extensive sand bodies that reflect sustained fluvio-deltaic sedimentation across the field. The A–B correlation panel illustrates consistent reservoir tops and bases across the wells, with low gamma-ray values and high resistivity responses confirming laterally persistent, clean sands charged with hydrocarbons (Fig. 3). Mild thinning of sand thickness is observed in the southeastern extent of SAM-1, suggesting subtle depositional heterogeneity. This continuity is consistent with

models of Niger Delta channel sands described by Weber (1987), where sand-rich channel belts extend over large lateral distances with localized shale drapes that impart internal heterogeneity but not full reservoir isolation.

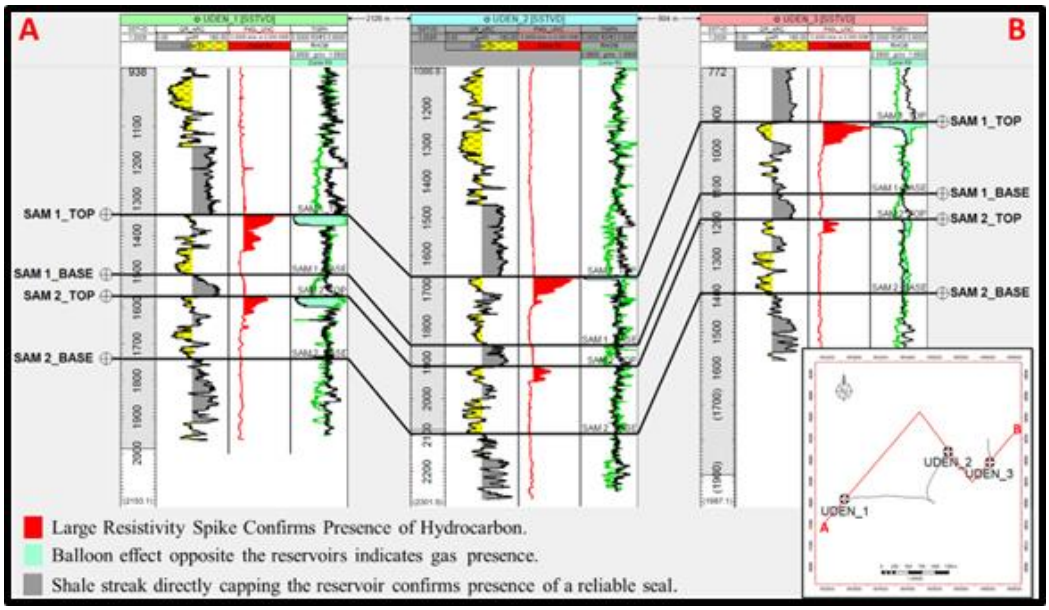

Fig.3: A to B correlation of hydrocarbon bearing sand across wells in the "UDEN" field. (Large resistivity spikes indicates presence of hydrocarbon)

Petrophysical evaluation confirms that both units possess excellent reservoir quality. SAM-1 exhibits average porosity of approximately 25%, low water saturation near 15%, and a net-to-gross ratio exceeding 0.7 (Fig. 4), while SAM-2 displays comparable porosity of about 23%, slightly higher Sw around 21%, and NTG close to 0.76 (Fig. 5). These values exceed the typical cutoffs for productive Niger Delta reservoirs (Ejedawe et al., 1984). Slight variations in porosity and Sw between wells suggest internal facies differentiation such as channel-axis to channel-margin transitions. These variations correspond well with multi-well interpretations demonstrating locally higher porosity and lower Sw in UDEN-2, which appears to represent a more proximal depositional setting relative to UDEN-1 and UDEN-3.

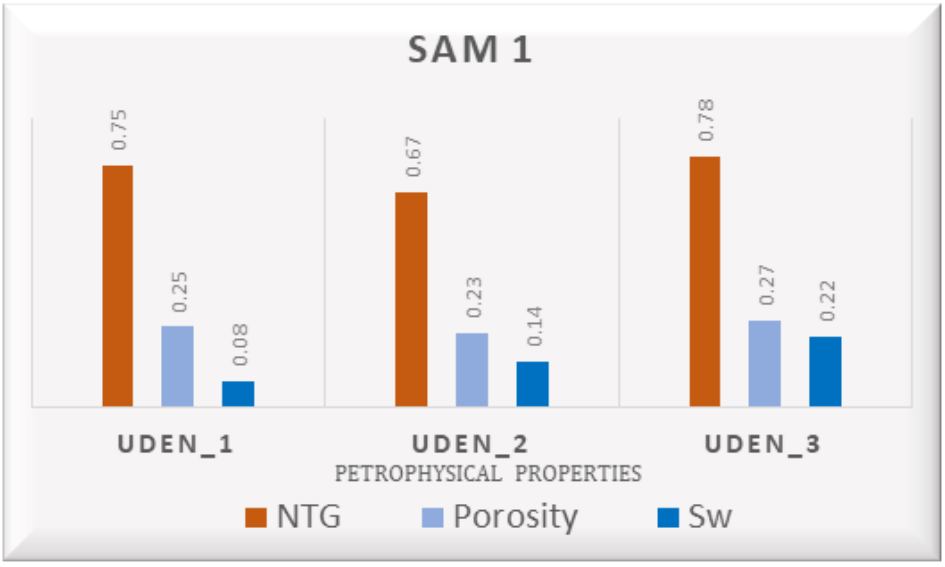

Fig. 4: A plot showing distribution of petrophysical properties in SAM 1 across the three wells

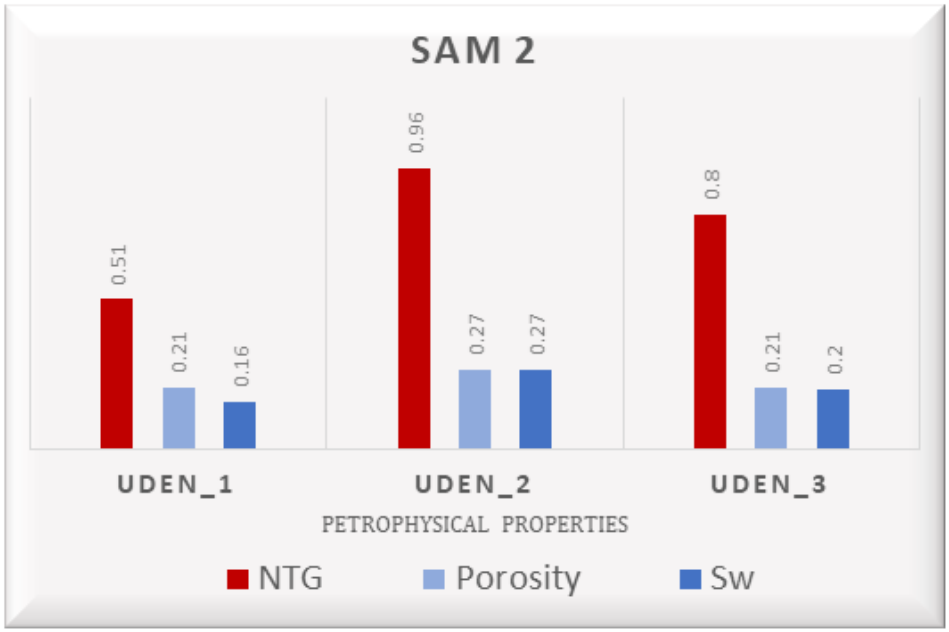

Fig 5: A plot showing distribution of pay thickness in SAM 2 across the three wells

The synthetic seismogram and well-to-seismic tie show excellent reflector alignment between log-derived acoustic impedance contrasts and seismic events (Fig. 6), strengthening confidence in seismic-derived horizon tracking and reservoir boundary identification. The dominant reflection polarity confirms sharp shale - sand impedance transitions typical of Niger Delta shallow marine and fluvial sands. This strong seismic-to-well tie ensures that interpreted reflectors accurately represent lithological boundaries in the subsurface, consistent with established standards described by Ekefre et. al. (2025).

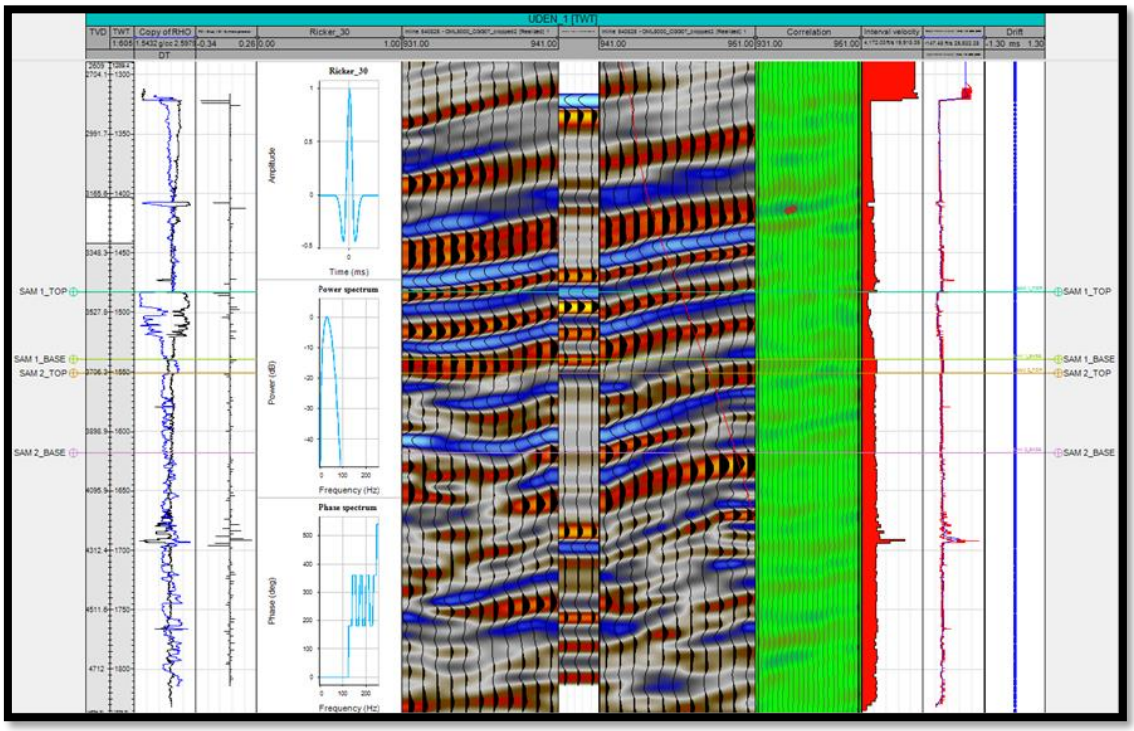

Fig. 6: Synthetic Seismogram generated for Uden field

Fault interpretation using variance attribute volumes revealed a complex fault system trending NE–SW and NW–SE (Fig. 7), characteristic of extensional tectonics in the Niger Delta growth-fault province. A total of sixty-two faults were interpreted, including major listric growth faults and antithetic splays, with throws ranging from roughly 10–60 meters. SAM-2 appears more compartmentalized by smaller branching faults, suggesting a more fragmented pressure communication system, while SAM-1 shows larger faults but fewer internal splays. These fault arrays are consistent with the compartmentalization models attributed to deltaic sand sequences affected by soft-sediment deformation and growth faulting (Umunna et al., 2019).

Time-structure maps of both SAM-1 and SAM-2 reveal multiple structural closures associated with rollover anticlines adjacent to major growth faults (Figs. 8a–b). Subsequent time-to-depth conversion using a check shot-derived velocity model (Fig. 9) confirms that the observed structural highs represent valid subsurface closures (Figs. 10a–b) with clear fault-bound trapping geometries. SAM-2 displays a particularly robust central structural closure forming the basis of Prospect X, where contour tightening indicates significant vertical relief and potential for hydrocarbon entrapment.

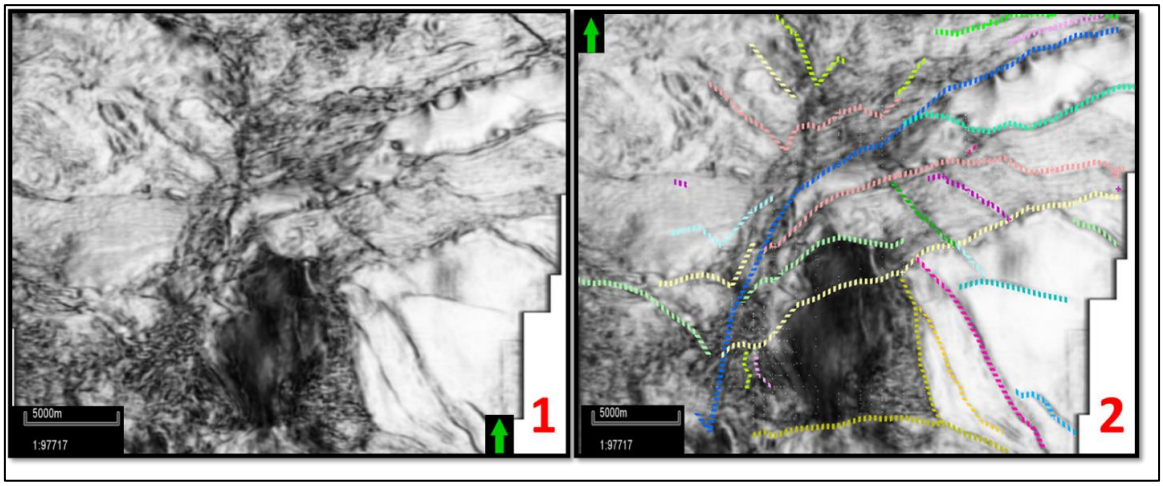

Fig. 7: Variance time slice (1200 ms) showing interpreted fault network (annotated) and structural compartments of Uden Field

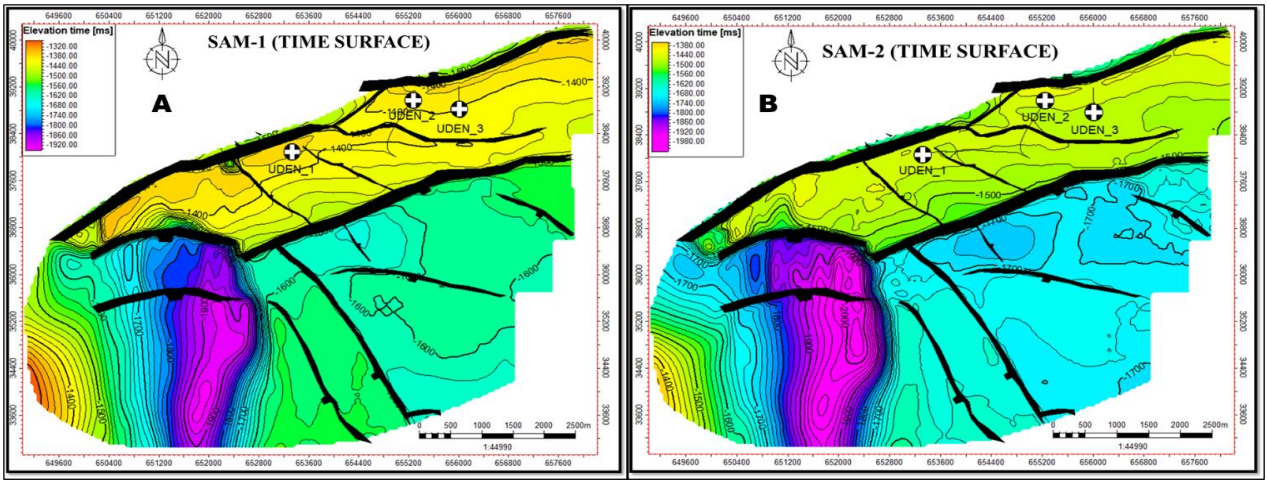

Fig. 8: Time Structure Map of SAM-1 (A) and SAM-2 (B) Horizon Showing Structural Highs, Growth Faults, and Well Locations in the Uden Field

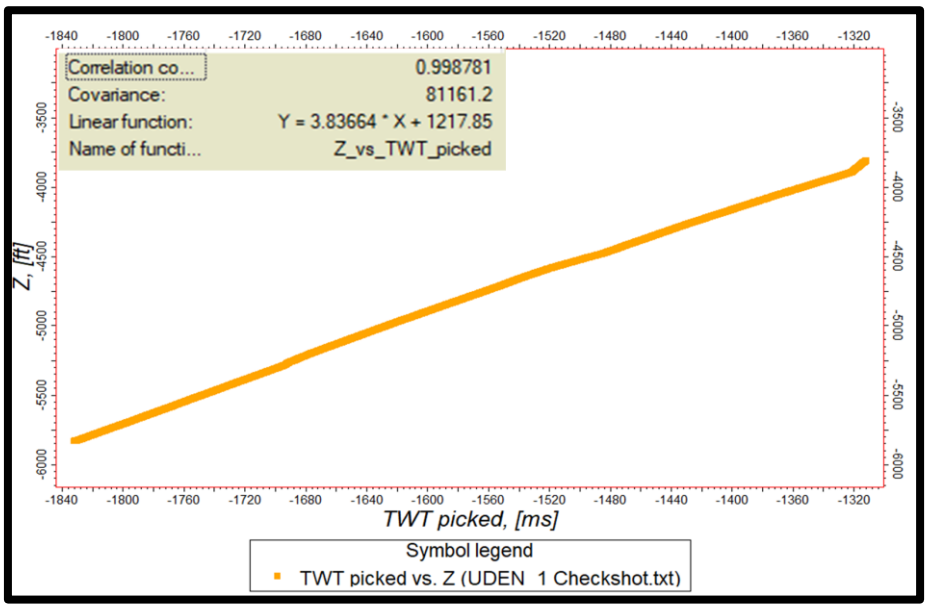

Fig. 9: Velocity model showing the time to depth relationship used in converting the time to depth maps

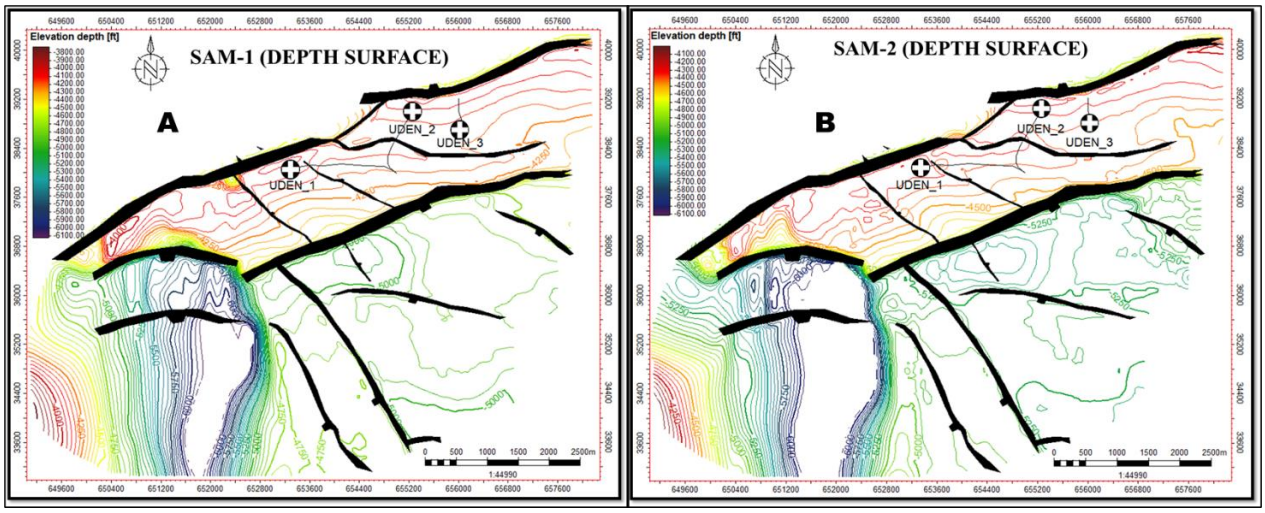

Fig 10: Depth Structure Map of SAM-1 (A) and SAM-2 (B) Horizon Showing Structural Closure, Fault Boundaries, and Well Locations

Seismic attribute analysis further supports the structural interpretation. RMS amplitude, maximum amplitude, magnitude, and average magnitude extractions reveal bright anomalies over both reservoirs (Figs. 11–14). These amplitude features coincide spatially with mapped structural highs and correlate with known hydrocarbon-bearing zones penetrated by wells. However, recognizing that amplitude anomalies can arise from tuning effects and lithologic variations (Chopra & Marfurt, 2007), attribute interpretation was constrained by well log data to avoid amplitude misinterpretation. The strongest amplitude conformance consistently aligns with the closure at Prospect X (Fig. 16), reinforcing its potential as a high-confidence target.

Lead identification within SAM-1 resulted in four potential leads (A–D) displaying partial structural closure and moderate seismic attribute expression (Fig. 15). In contrast, SAM-2 contains the more compelling Prospect X (Fig. 16), exhibiting clear four-way dip closure and continuous amplitude presence consistent with trapped hydrocarbons. The integration of structural mapping, attribute response, and petrophysical data strengthens confidence in Prospect X as a priority drilling candidate for incremental field development.

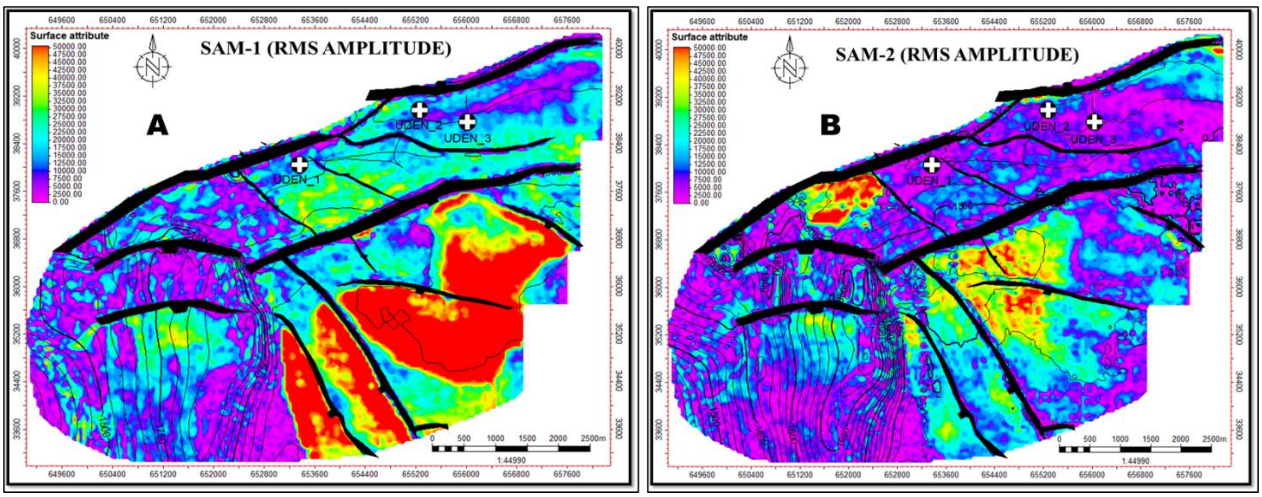

Fig. 11: RMS Amplitude Map of SAM-1 (A) and SAM-2 (B) Horizon Highlighting High-Energy Zones Associated with Potential Hydrocarbon Accumulations

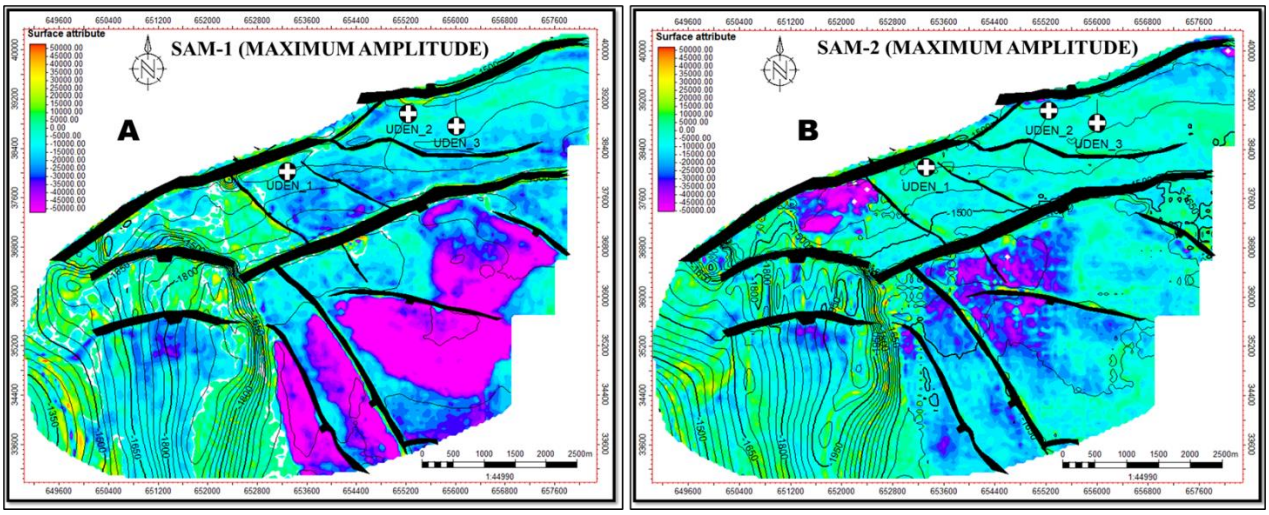

Fig. 12: SAM-1 (A) and SAM-2 (B) Maximum Amplitude Map Indicating Peak Reflectivity Zones Along Structural Highs

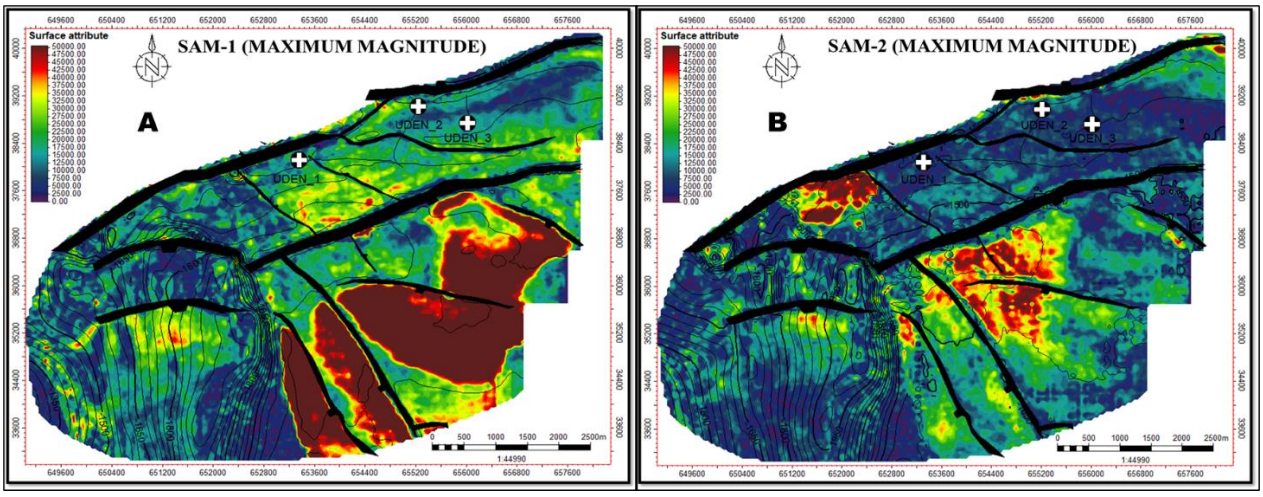

Fig. 13: Maximum Magnitude Map Showing Absolute Peak Amplitude Strengths Across the SAM-1 (A) and SAM-2 (B) Reservoir

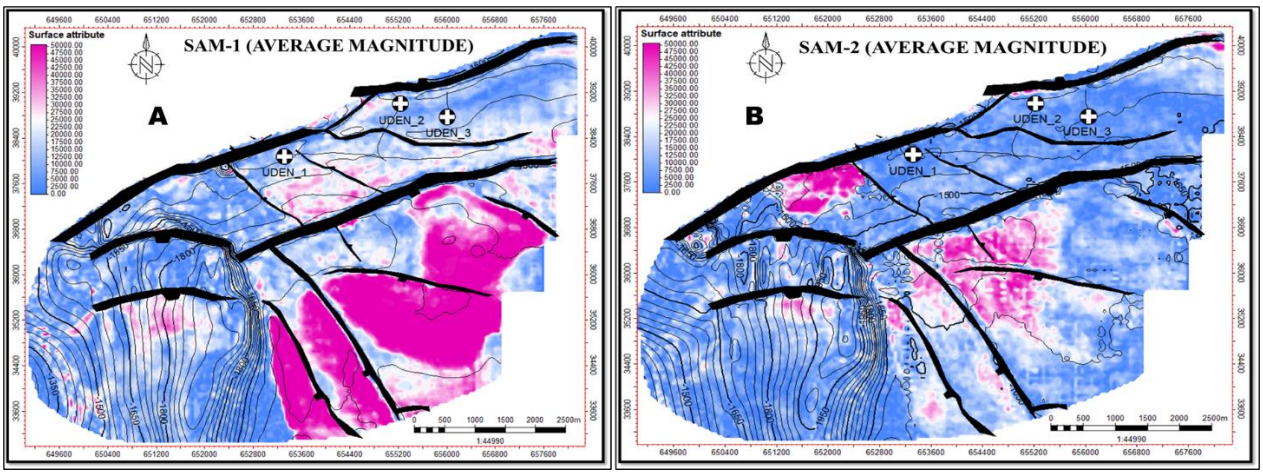

Fig 14: SAM-1 (A) and SAM-2 (B) Average Magnitude Map Reflecting Spatial Distribution of Mean Reflectivity Across the Reservoir Interval

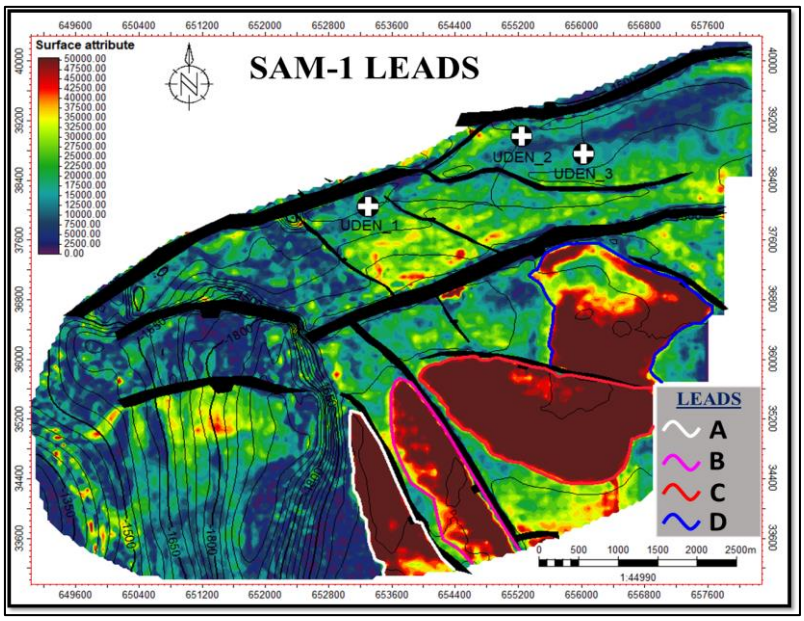

Fig. 15: Seismic attribute map (maximum magnitude) within the SAM-1 interval showing identified leads.

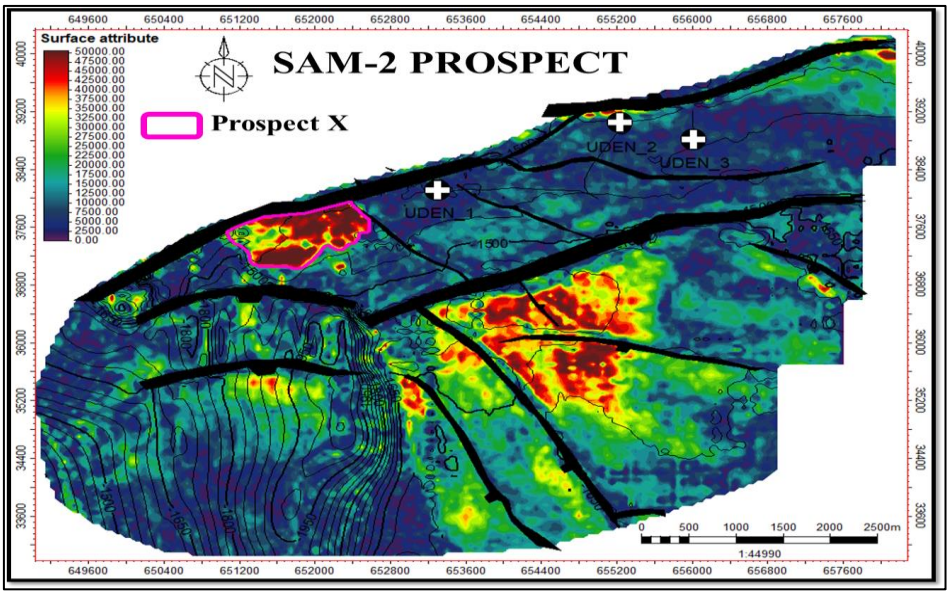

Fig. 16: Seismic attribute map (maximum magnitude) within the SAM-2 interval showing the identified prospect

Deterministic volumetric analysis for SAM-1 and SAM-2 indicates a Stock Tank Oil Initially in Place (STOIIP) of approximately 141 MMbbl and 157 MMbbl, respectively, while Prospect X contributes an additional 133.7 MMbbl. Probabilistic Monte Carlo simulations yielded STOIIP distributions of ~118–142–181 MMbbl for SAM-1 and ~124–160–203 MMbbl for SAM-2, corresponding to P90, P50, and P10 confidence limits (Fig. 17). These distributions indicate that SAM-1 is volumetrically more certain, whereas SAM-2 possesses greater upside capacity but also structural uncertainty due to fault segmentation, consistent with reservoir evaluation frameworks described by Rose (2001).

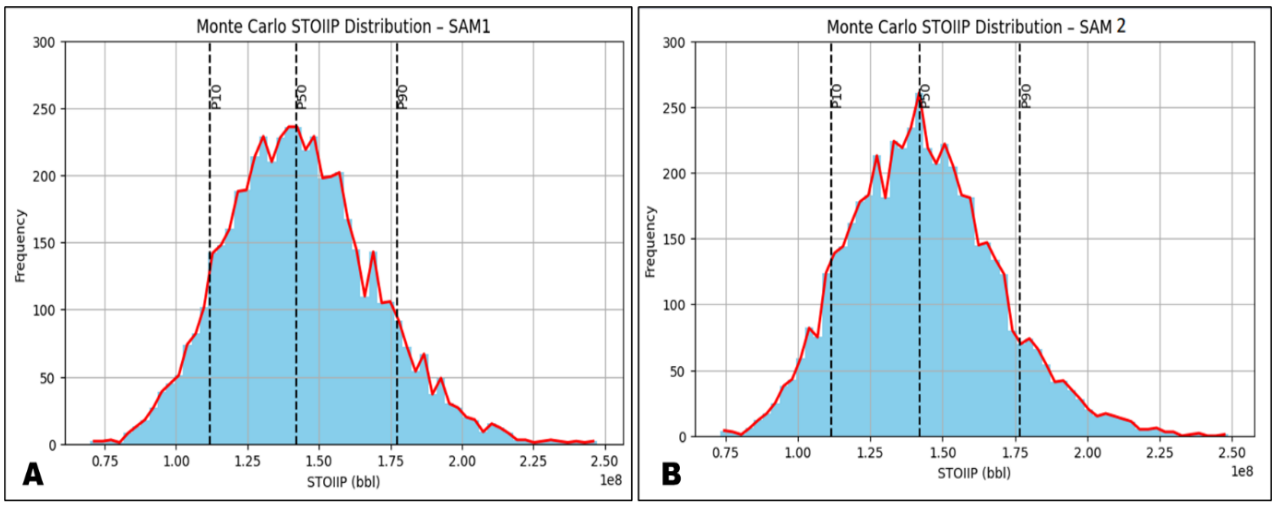

Fig. 17: Plot showing the probability STOIIP distribution in SAM-1(A) and SAM-2 (B) reservoir

Comparison of STOIIP estimates with cumulative production of ~42.9 MMbbl indicates recovery factors of ~30.2% for SAM-1 and ~27.3% for SAM-2 (Fig. 18). The lower recovery of SAM-2 reflects the significant role of structural segmentation in limiting lateral drainage efficiency. Based on P50 STOIIP values, remaining oil-in-place is ~99 MMbbl for SAM-1 and ~114 MMbbl for SAM-2, giving a combined unrecovered total of approximately 213 MMbbl. Much of this bypassed oil is likely sequestered in isolated compartments behind partially sealing growth faults, consistent with field behavior documented by Jubril and Amajor (1991).

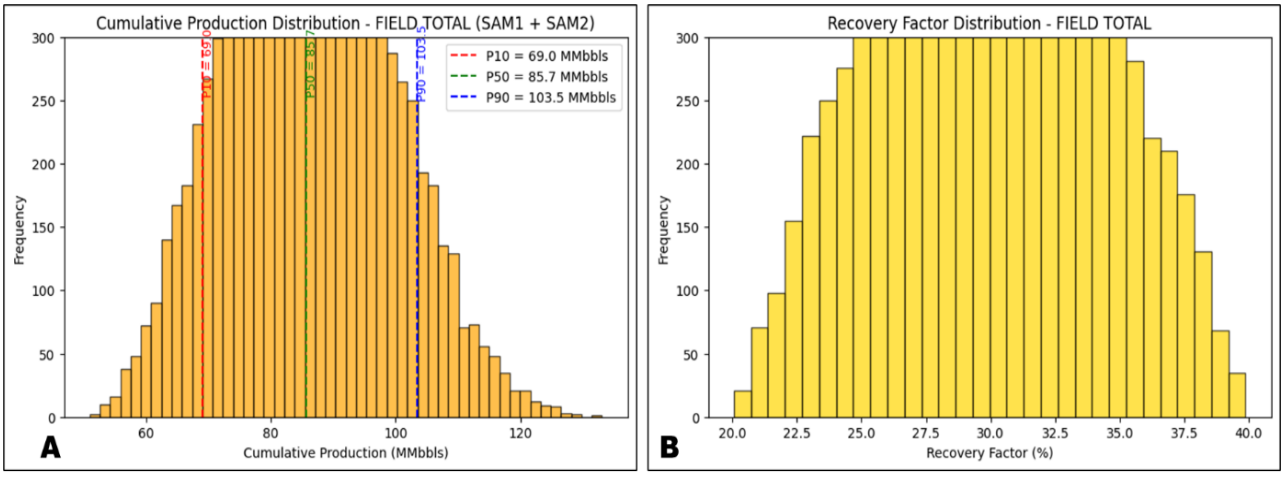

Fig. 18a: Bar chart comparing STOIIP versus cumulative production for SAM1 and SAM 2 reservoirs **(b):** Recovery factor comparison for both reservoirs.

By integrating recovery performance, STOIIP probability distribution, and reservoir segmentation indicators, a bypassed hydrocarbon screening workflow was carried out using specific screening criteria including recovery factor thresholds, structural compartmentalization, and volumetric uncertainty. The screening approach required that intervals demonstrating low recovery relative to P50 STOIIP values, evidence of fault-bounded segmentation, or weak completion penetration be flagged as bypassed candidates. Under these criteria, SAM-1, despite exhibiting a moderately acceptable recovery factor, still shows significant bypassed oil volumes, estimated between 71 MMbbl (P10) and 121.5 MMbbl (P90) (Table 2a). This indicates that thin-bedded sand units below log resolution, lateral facies variations, or incomplete completion coverage may have prevented full reservoir sweep, allowing pockets of unrecovered oil to remain within the reservoir.

SAM-2 was consistently classified as bypassed under all screening thresholds particularly because its actual recovery factor fell below the minimum acceptable recovery-to-STOIIP ratio defined in the screening criteria. Its remaining oil volumes of 71 MMbbl (P10), 99.4 MMbbl (P50), and 121.1 MMbbl (P90) (Table 2b) underscore the influence of poor lateral connectivity and structural segmentation. The higher volumetric uncertainty envelope and stronger structural compartmentalization of SAM-2 further justify its classification as under-drained. The combined assessment in Table 2c across both reservoirs indicates substantial remaining hydrocarbon potential when evaluated against the defined bypassed-oil screening parameters. These findings highlight the technical need for targeted optimization approaches such as fault-assisted infill drilling, zonal recompletion of undrained intervals, and enhanced subsurface surveillance (e.g., pressure transient analysis, production logging, and time-lapse seismic monitoring) to improve overall recovery and mobilize the unswept hydrocarbons still resident within SAM-1 and SAM-2.

Table 2a: Bypassed hydrocarbon screening results for SAM1 reservoir

SAM 1					
	STOIIP (bbls)	Cum. Prod. (bbls)	RF (%)	Remaining Oil (bbls)	Bypassed Flag
P10	111,940,685	30,800,000	27.51	81,140,685	Bypassed Candidate
P50	141,963,473	42,900,000	30.22	99,063,473	
P90	177,394,341	55,900,000	31.51	121,494,341	

Table 2b: Bypassed hydrocarbon screening results for SAM 2 reservoir

SAM 2					
	STOIIP (bbls)	Cum. Prod. (bbls)	RF (%)	Remaining Oil (bbls)	Bypassed Flag
P10	111,565,087	30,800,000	27.61	80,765,087	Bypassed Candidate
P50	141,945,108	42,500,000	29.94	99,445,108	
P90	176,814,035	55,700,000	31.50	121,114,035	

Table 2c: Combine bypassed hydrocarbon Volumes for SAM-1 and SAM-2 reservoir

FIELD TOTAL					
	STOIIP (bbls)	Cum. Prod. (bbls)	RF (%)	Remaining Oil (bbls)	Bypassed Flag
P10	223,505,772	61,600,000	27.56	161,905,772	Bypassed Candidate
P50	283,908,581	85,400,000	30.08	198,508,581	
P90	354,208,376	111,600,000	31.51	242,608,376	

5.0 Discussion

The integrated well-log correlations, seismic interpretation, and attribute analysis provide a clearer understanding of reservoir behavior in the Uden Field. The laterally persistent but internally heterogeneous sands identified from well logs (Fig. 3) are consistent with the fluvio-deltaic depositional model of the Niger Delta described by Doust & Omatsola (1990) and Reijers (2011). The presence of interbedded shale streaks observed in the gamma-ray and resistivity logs (Fig. 3) supports earlier findings by Weber (1987), who emphasized that heterolithic bedding strongly influences reservoir continuity within the Agbada Formation.

Amplitude-based seismic attributes (RMS, maximum amplitude, and magnitude) reveal high-reflectivity zones corresponding to clean, hydrocarbon-bearing sands (Figs. 11). This relationship aligns with the attribute–fluid interpretations discussed by Chopra and Marfurt (2007) and is consistent with Niger Delta studies by Adeoye and Enikanselu (2009), who reported strong amplitude anomalies as reliable indicators of high-quality channel sands.

The discontinuities and lineaments extracted from coherence and dip-variance attributes given in Fig 7 indicate the presence of subtle faults and structural breaks. These features resemble the sub-seismic fault networks described by Avbovbo (1978) and Umunna et al. (2019), both of whom noted that minor structural elements significantly influence compart-mentalization and recovery efficiency within Niger Delta reservoirs.

The performance contrast between SAM1 and SAM2 reflects the geological variability observed in both datasets. SAM1 demonstrates more continuous sands and coherent attribute patterns (Figs. 11-14), resulting in a recovery factor of approximately 30%, which is within the typical Niger Delta range of 20–35% reported by Ejedawe (1984) and Weber (1987). In contrast, SAM2 exhibits more segmented attribute patterns (Figs. 11b-14b), indicative of compartmentalization that likely contributes to its lower recovery (~27%). This observation agrees with findings by Jubril et al. (1991), who noted that rapid facies transitions and shale drapes frequently reduce sweep efficiency in deltaic reservoirs.

The Monte Carlo volumetric distribution (Fig. 17) shows a wide P10–P90 spread, highlighting uncertainty driven by reservoir heterogeneity. This outcome aligns with the recommendations of Rose (2001), who emphasized the need for probabilistic analysis in geologically complex settings. The bypassed hydrocarbon screening in Table 2c further indicate remaining oil in structurally or stratigraphically isolated zones in both SAM1 and SAM2, consistent with observations by Ejedawe (1981) and Adeoye & Enikanselu (2009) regarding the persistence of unswept hydrocarbons in compartmentalized Niger Delta fields.

Seismic attribute mapping identifies undrilled high-amplitude closures (Prospect X) in SAM2 (Fig. 16). Similar attribute-guided prospect identification has been demonstrated by Onuoha and Ofoegbu (1988), who reported that attribute-supported drilling significantly improves the detection of unpenetrated reservoir compartments.

Overall, the Uden Field exhibits reservoir characteristics consistent with regional Niger Delta studies: volumetrically significant sands affected by internal heterogeneity and structural segmentation. The integrated interpretation highlights opportunities for improved field development through targeted infill drilling, attribute-guided well placement, and optimized re-completion strategies. These approaches long recommended by Weber (1987) and Umunna et al. (2019) to enhance recovery and mitigate bypassed hydrocarbons.

6.0 Summary and Conclusion

This study applied an integrated workflow combining well-log correlation, petrophysical evaluation, 3D seismic interpretation, seismic

attribute analysis, and both deterministic and probabilistic volumetric assessment to evaluate reservoir performance and bypassed hydrocarbons in the Uden Field, Niger Delta. Two main reservoirs, SAM-1 and SAM-2, were mapped within the Agbada Formation and exhibit excellent reservoir quality, characterized by high porosity (0.23–0.25), net-to-gross ratios >0.70, and low water saturation (<0.25). Structural interpretation reveals a fault-controlled system dominated by growth faults and rollover geometries, while amplitude-based seismic attributes effectively delineate hydrocarbon-prone zones. Four leads in SAM-1 and one well-defined prospect (Prospect X) in SAM-2 were identified. Deterministic and probabilistic volumetric assessments indicate mid-case STOIIP values of ~142 MMbbl per reservoir, with Monte Carlo simulations capturing realistic uncertainty ranges (111–177 MMbbl). Estimated recovery factors (SAM-1: ~30%; SAM-2: 27–29%) demonstrate the presence of significant bypassed hydrocarbons (up to ~121 MMbbl), highlighting the potential for optimized development strategies.

The results of this research provide important insights into reservoir characterization in structurally complex Niger Delta settings. This study is novel in its integrated application of seismic attributes, petrophysical evaluation, and probabilistic volumetric modeling to quantify bypassed hydrocarbons in a structurally complex Niger Delta field. Unlike previous Niger Delta studies, it combines deterministic STOIIP, Monte Carlo simulations, and attribute-supported screening to identify under-drained compartments and rank prospects for optimized recovery.

Key conclusions are:

1. **Reservoir Quality and Continuity:** SAM-1 and SAM-2 form laterally extensive fluvio-deltaic sand systems with consistently high-quality reservoir properties.
2. **Structural Control:** Growth faults and rollover anticlines act as effective trapping mechanisms, with SAM-2 showing significant structural closure and compartmentalization effects.
3. **Seismic Attribute Utility:** RMS and maximum amplitude attributes successfully delineated hydrocarbon-bearing zones and correlated well with petrophysical evidence, demonstrating their effectiveness in reservoir prediction.
4. **Probabilistic Volumetric Assessment:** Monte Carlo simulations provide reliable uncertainty bounds for STOIIP (111–177 MMbbl), enabling more informed decisions in reservoir management and field development.
5. **Bypassed Hydrocarbons:** Both reservoirs contain substantial remaining oil volumes, confirming the need for targeted infill drilling, re-completions, and potential EOR applications.
6. **Exploration and Development Upside:** The clear delineation of Prospect X in SAM-2 and four additional leads in SAM-1 presents a significant opportunity for incremental hydrocarbon recovery and future drilling campaigns.

References

Adeoye, T. O. & Enikanselu, P. A. (2009). Reservoir Characterization of 'Laja' Oil Field, Niger Delta. The Pacific Journal of Science and Technology, 10(1), 604-617.

Siddiqui, M., Al-Yateem, K. & Al-Thawadi, A. (2007). A New Tool to Evaluate the Feasibility of Petroleum Exploration Projects Using a Combination of Deterministic and Probabilistic

Methods. SPE Middle East Oil & Gas Show and Conference.

Akpan, A. E., Ekwok, S. E., Ben, U. C., Ebong, E. D., Thomas, J. E., Ekanem, A. M., George, N. J., Abdelrahman, K., Fnais, M. S., Eldosouky, A. M., Andráš, P., & Alarifi, S. S. (2023). Direct Detection of Groundwater Accumulation Zones in Saprock Aquifers in Tectono-Thermal Environments. *Water*, *15*(22), 3946. https://doi.org/10.3390/w15223946

Akpan, A.S. Obiora, D.N Okeke, F.N, Ibuot, J.C.& George, N.J (2020). Influence of wavelet phase rotation on post stack model based seismic inversion: A case study of X-field, Niger Delta, Nigeria, *Journal of Petroleum and Gas Engineering*, 11(1), 57-67

Akpan, A.S., Okeke, F.N., Obiora, D.N. & George, N.J. (2021). Modelling and mapping hydrocarbon saturated sand reservoir using Poisson's impedance (PI) inversion: a case study of Bonna field, Niger Delta swamp depobelt, Nigeria. *J Petrol Explor Prod Technol* **11**, 117–132 (2021). https://doi.org/10.1007/s13202-020-01027-8

Akpan, M. J., George, N.J. Ekanem, A.M.& Nathaniel, E.U (2023). Deploying Geostatistical Stochastic Inversion Modeling in The Characterization of Reservoirs: A Case Study from an Onshore Niger *Delta Field. Malaysian Journal of Geosciences, 7(2): 87-95*

Akpan, M.J., George, N.J., Ekanem, A.M. & Ekong, U.N. (2025). Petrophysical appraisal and 3-D structural interpretation of reservoirs in an Onshore Niger Delta Field, Southeastern Nigeria, International Journal of Energy and Water Resources, 9(1), 89-101

Avbovbo, A. A. (1978). Tertiary lithostratigraphy of Niger Delta. *AAPG Bulletin*, *62*(2), 295–306.

Burke, K., Dessauvagie, T. F. J., & Whiteman, A. J. (1971). The opening of the Gulf of Guinea and the geological history of the Benue Depression and Niger Delta. *Nature Physical Science*, *233*, 51–55.

Chopra, S. & Marfurt, K. J. (2007). Seismic Attributes for Prospect Identification and Reservoir Characterization. SEG Geophysical Developments Series No. 11. Society of Exploration Geophysicists.

Doust, H., & Omatsola, E. (1990). Niger Delta. In Divergent/passive Margin Basins (pp. 239–248). AAPG Memoir 48.

Ebong, S.T., Ekanem, A.M. & George, N.J. (2023). Fluid prediction through lithological analysis in '**M**' oil field Niger Delta: using rock physics approach, *Malaysian journal of Geosciences, 7(1), 55-61*

Ejedawe, J. E., Okoye, N. V., & Olayinka, O. (1984). Hydrocarbon habitat of the Niger Delta. *AAPG Bulletin*, 68(3), 371–386.

Ejedawe, J.E. (1981). *Patterns of hydrocarbon distribution in the Niger Delta basin*. American Association of Petroleum Geologists Bulletin, 65(9), pp. 1574–1585.

Ekanem, A.M., George, N.J., Thomas, J.E. & Ekpenyong, N.E (2021). Seismic modelling study of CO2 effects on P-wave amplitude, *Modeling Earth Systems and* Environment, 7(3), 1693-1701, https://doi.org/10.1007/s40808-020-00904-9

Ekefre, A. E., George, N. J., Udoh, A. C., Harry, T. A., & Etim, C. E. (2025). Predictive Analysis of Sand Production and Flow Implications using Petrophysical-Geomechanical Properties: A case of "ANY" Field, Niger Delta. *Researchers Journal of Science and*

Technology, *5*(2), 54–73. Retrieved from https://rejost.com.ng/index.php/home/article/view/174

Evamy, B. D., Haremboure, J., Kamerling, P., Knaap, W. A., Molloy, F. A., & Rowlands, P. H. (1978). Hydrocarbon habitat of Tertiary Niger Delta. AAPG Bulletin, 62(1), 1–39.

Fahrezi, O., Boni, S., Dyah R. R. (2022). Uncertainty Assessment for Field Development Study Using Monte Carlo Simulation on Salap Field Multilayer Gas Reservoir, *Journal of Petroleum and Geothermal Technology*, 3(1), 2723-1496

Gao, D. (2013). Latest developments in seismic attribute analysis. *The Leading Edge*, 32(6), 614–622. https://doi.org/10.1190/tle32060614.1

Horsfall, O.I., Akpan, M.J. & George, N.J. (2024). Reservoir characterization of GABO field in the Niger Delta Basin using facies and petrophysical analyses, *Results in Earth Sciences 2*, 100038, https://doi.org/10.1016/j.rines.2024.100038

Jubril, M. A., & Amajor, L. C. (1991). The Afam Clay Member: a Lower Miocene incised channel in the south-eastern Niger Delta**.** *Marine and Petroleum Geology***,** *8*(2), 163–173.

Morgan, R. (2004). Structural controls on the positioning of submarine channels on the lower slopes of the Niger Delta. *Geological Society, London, Memoirs*, *29*, 45–51.

Obianwu, V.I, Udoh, J.T., George, A.M. & George, N.J. (2015). Seismic Early Warning Foundation Conditions Evaluation Survey for Civil Engineering Constructions in Akpabuyo Local Government Area of Cross River State, Nigeria, *British Journal of Applied Science & Technology 6(6), 583*

Onuoha, K. M., & Ofoegbu, C. O. (1988). Subsidence and evolution of Nigeria's continental margin: implications of data from Afowo-1 well**.** *Marine and Petroleum Geology***,** *5*(2), 175–181.

Reijers, T. J. A. (1996). *Selected chapters on geology: Sedimentary geology, sequence stratigraphy, and petroleum geology of the Niger Delta*. Shell Petroleum Development Company.

Reijers, T.J.A. (2011). *Stratigraphy and sedimentology of the Niger Delta*. Geologos, 17(3), pp. 133–162.

Rose, P. R. (2001). Risk analysis and management of petroleum exploration ventures: A synthesis**.** In R. K. Merrill, G. D. Taylor, & B. C. Dodson (Eds.), *Verification of petroleum reservoir engineering evaluations* (Vol. 44, pp. 31–41). AAPG Special Volume.

Short, K. C., & Stauble, A. J. (1967). Outline of geology of Niger Delta. *AAPG Bulletin*, *51*(5), 761–779.

Taner, M. T., Koehler, F., & Sheriff, R. E. (1979). Complex seismic trace analysis. *Geophysics*, *44*(6), 1041–1063. https://doi.org/10.1190/1.1440994.

Udo, K. I, George, N. J., Akankpo, A. O., Azuoko, & Aka, M. U. (2020) Determining fracture pressure gradients from well logs, *international journal of advanced geosciences 8 (1), 5-9*

Umoren, E.B. & George, N.J. (2018). Time lapse (4D) and AVO analysis: A case study of Gullfaks field, Northern North Sea, NRIAG Journal of Astronomy and Geophysics, 7(1), 62-77, https://doi.org/10.1016/j.nrjag.2018.03.004

Umunna, O., Uko, E. D., & Akpabio, I. O. (2019). Delineation of Subsurface Structures in Toja Field in the Niger Delta Using Well-Logs and Seismic Data. *Malaysian Journal of Geosciences (MJG)*, *3*(2), 43-51.

Weber, K. J. (1987). Hydrocarbon distribution patterns in Nigerian growth fault structures controlled by structural style and stratigraphy. *Journal of Petroleum Science and Engineering*, *1*(1), 91–104.

Weber, K. J., & Daukoru, E. M. (1975). Petroleum geology of the Niger Delta. *Proceedings of the 9th World Petroleum Congress*, *2*, 210–221.